A Hybrid Numerical Method for High Contrast Conductivity Problems

Liliana Borcea*, and George C. Papanicolaou†

June 10, 1997

Abstract

We introduce and test extensively a numerical method for computing efficiently current flow in media with high contrast conductivity. This method combines our analytical understanding of the form of the flow field near narrow channels with standard numerical methods elsewhere in the flow regime and so it is a hybrid numerical method.

Keywords: high contrast conductivity, resistor networks, hybrid numerical methods

1 Introduction

Natural porous media exhibit strong spatial variability in most of their properties, such as hydraulic conductivity, electrical conductivity, dielectric permeability, etc, even on mesoscopic length scales where some averaging has been incorporated into the modeling. Mathematically this means that we have to solve partial differential equations with coefficients that take very large and very small values in the domain.

Forward problems for such partial differential equations pose difficult analytical and computational questions. In numerical computations one needs very fine meshes to capture the correct behavior of flow properties of the high contrast medium and this leads to large and ill conditioned matrices that must be inverted. Consequently, iterative methods used in matrix inversion have very poor convergence rates.

In this paper we develop a numerical method for high contrast conductivity problems which avoids the difficulties encountered by other methods by combining standard numerical schemes with our analytical understanding of flow channeling [11, 5] based on asymptotic methods. Flow channeling in media with high contrast conductivity was studied before. Keller [10] and Batchelor and O'Brien [3] show that flow in media with high contrast conductive or resistive inclusions concentrates in narrow channels or gaps in between the inclusions. However, their analysis is based on assumptions about the shape of the inclusions. Our hybrid numerical method has been constructed with imaging applications in mind where the shape of the inclusions is not known beforehand. In these applications it is convenient to assume that the high contrast arises in a simple, generic manner as a continuum [6]. Thus, we model the high contrast hydraulic conductivity $K(\mathbf{x})$ by

$$K(\mathbf{x}) = K_0 e^{-\frac{S(\mathbf{x})}{\epsilon^2}}, \tag{1.1}$$

*Applied Mathematics, Caltech 217-50, Pasadena, CA 91125, email: borcea@ama.caltech.edu

†Dept of Mathematics, Stanford University, Stanford, CA 94305, email: papanico@math.stanford.edu

where K_0 is a reference constant conductivity, $S(\mathbf{x})$ is a smooth function and ϵ is a small parameter. Variations of the function $S(\mathbf{x})$, the scaled logarithm of the conductivity, are amplified by the parameter ϵ in (1.1), producing the high contrast of the hydraulic conductivity.

Conductivities of form (1.1) were used before in the analysis of flow properties of media with high contrast [11, 5, 8] and these studies show that the flow concentrates around regions where the conductivity has saddle points. Channels of strong flow near saddle points of the conductivity (1.1) are generalizations of the channels or gaps in high contrast media with conductive or resistive inclusions.

In many applications we do not know precisely the local conductivity $K(\mathbf{x})$. We know it only approximately. In [5] we show that when the medium has high contrast, only a limited amount of information about the local conductivity is needed for obtaining a good estimate of overall quantities like the effective conductivity. The regions in the heterogeneous medium that really matter are those where channels of strong flow develop. Thus, it is important that the flow in the channels is computed correctly. In general, in the vicinity of a channel, the conductivity $K(\mathbf{x})$ is not a smooth function as (1.1) implies. However, as in [6], we can model the local conductivity $K(\mathbf{x})$ in the vicinity of a channel by a smooth function of form (1.1) and obtain a good estimate of the overall flow behavior in the domain of interest. These conclusions are based on the results obtained for the inverse problem of inferring the conductivity in a domain from boundary measurements (see [6]).

The flow channeling that develops at saddle points of the conductivity (1.1) leads to a resistor network approximation of the high contrast medium (see [5]). However, the network approximation is just the leading order term in the asymptotic approximation of the flow in the high contrast medium. In physical problems where the contrast is finite and there are, in addition, regions of weak flow concentration, direct use of the asymptotics produces rather crude results. Our hybrid numerical method uses the asymptotic theory in regions where strong channeling develops, while standard numerical schemes are used elsewhere in the flow regime.

The paper is organized as follows. In section 2 we formulate the problem, in section 3 we describe the hybrid method and in section 4 we test its performance in several situations and compare it to computations with standard numerical schemes as well as with the adaptive schemes of [2].

2 Formulation of the problem

We consider the isotropic steady state flow problem

$$-\nabla \cdot [K(x,y)\nabla\phi(x,y)] = f(x,y) \tag{2.1}$$

defined in a unit square domain Ω (see fig. 2.1), where K is the hydraulic conductivity, $\phi(x,y)$ is the hydraulic head and $f(x,y)$ is the recharge. We choose a simple domain in order to simplify the exposition of the hybrid method but the methodology presented in this paper applies to regions Ω of any shape.

The flux is obtained from Darcy's law $\mathbf{j} = -K\nabla\phi$ and the flow can be driven by either the forcing term $f(x,y)$ or by some inhomogeneous boundary conditions. In order to fix ideas we assume that the flow is confined in Ω and impose the no-flux boundary conditions

$$\frac{\partial\phi}{\partial n}|_{\partial\Omega} = 0, \tag{2.2}$$

where $\mathbf{n}$ is the unit normal at the boundary, pointing outwards. The recharge $f(x,y)$ is prescribed so that the flux injected equals the one taken out. For example, for a point source at $\mathbf{x}_1$ and sink at $\mathbf{x}_2$ we take

$$f(x,y) = \delta(\mathbf{x}-\mathbf{x}_1) - \delta(\mathbf{x}-\mathbf{x}_2). \tag{2.3}$$

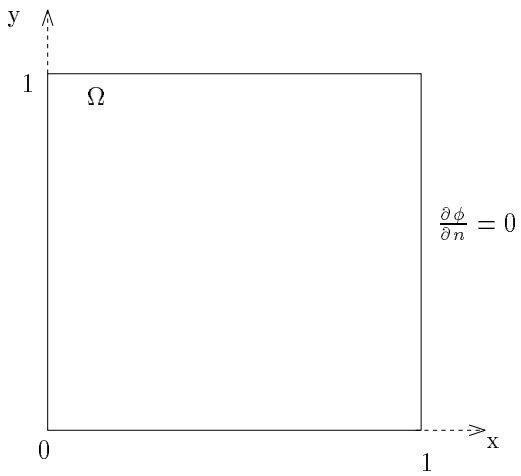

Figure 2.1: Computational domain

In the numerical computations we use an approximation of the recharge (2.3) where the delta functions are approximated by narrow Gaussians centered at $\mathbf{x}_1$ and $\mathbf{x}_2$. Problem (2.1)-(2.3) with $K(\mathbf{x}) > 0$ has a unique solution $\phi(x, y)$ up to an additive constant.

3 The numerical method

3.1 Review of the asymptotic theory

In this section we review some of the results obtained in [11, 5] which apply to problem (2.1)-(2.3) when the high contrast hydraulic conductivity is modeled by (1.1). The problem is analyzed by using asymptotic and variational techniques and the results show that the flow concentrates in small neighborhoods of saddle points of the hydraulic conductivity $K(\mathbf{x})$. Moreover, by using the variational formulation of the effective conductivity and resistance

$$\begin{aligned} \overline{K} &= \min_{<\nabla\phi>=\mathbf{e}} < K(\mathbf{x})\nabla\phi \cdot \nabla\phi > \\ \overline{K}^{-1} &= \min_{<\mathbf{j}>=\mathbf{e},\ \nabla\cdot\mathbf{j}=0} < \frac{1}{K(\mathbf{x})}\mathbf{j}\cdot\mathbf{j} >, \end{aligned} \tag{3.1}$$

it is shown that, in the asymptotic limit of infinitely high contrast, the leading order term in the effective conductivity $\overline{K}$ is obtained by considering the flow only in small neighborhoods of the saddle points of $K(\mathbf{x})$. In (3.1) $< \cdot >$ stands for the normalized average over Ω, $\mathbf{j}(\mathbf{x})$ is the flux and $\mathbf{e}$ is the unit vector in the direction of the average flow.

To give a brief review of the asymptotic theory we consider the local flow problem in the vicinity of a saddle point $\mathbf{x}_S \in \Omega$ of the conductivity. In a small neighborhood of the saddle point $\mathbf{x}_S$ the conductivity can be written as

$$K(\mathbf{x}) = K_0 e^{-\frac{S(\mathbf{x})}{\epsilon^2}} \approx K(\mathbf{x}_S) e^{\frac{k(x-x_S)^2}{2\epsilon^2} - \frac{p(y-y_S)^2}{2\epsilon^2}}, \tag{3.2}$$

where k and p are the curvatures of $S(\cdot)$ at the saddle point. In (3.2) we assume that the saddle point is oriented in the direction $\mathbf{e}_1$. In general, the saddle point can be oriented in any direction and equation (3.2) still holds if at $\mathbf{x}_S$ we introduce a local system of coordinates (x, y) such that

direction x coincides with the direction of the saddle. We take as the small vicinity of $\mathbf{x}_S$ the square $\mid x - x_S \mid \leq \delta, \mid y - y_S \mid \leq \delta$ where the parameter $\delta \to 0$ in such a way that $\frac{\delta}{\epsilon} \to \infty$ as $\epsilon \to 0$.

The local problem near the saddle point is

$$\begin{aligned} &\nabla \cdot \{K(\mathbf{x}_S) exp[\frac{k(x-x_S)^2}{2\epsilon^2} - \frac{p(y-y_S)^2}{2\epsilon^2}]\nabla\phi\} = 0 \quad \text{for} \mid x - x_S \mid < \delta \quad \text{and} \mid y - y_S \mid < \delta \\ &\nabla\phi \cdot \mathbf{n} = 0 \quad \text{for} \mid y - y_S \mid = \delta \\ &\phi = -C \quad \text{for } x = x_S + \delta \quad \text{and } \phi = C \quad \text{for } x = x_S - \delta, \end{aligned} \tag{3.3}$$

which we solve by separation of variables. The constant C in equation (3.3) determines how much flow goes through the saddle point and it depends on the driving condition $f(x, y)$ given by (2.3), the contrast of $K(\mathbf{x})$ and other factors. The solution of equation (3.3) is

$$\phi(\mathbf{x}) \approx -Cerf[\sqrt{\frac{k}{2\epsilon^2}}(x - x_s)]. \tag{3.4}$$

The analytical basis for (3.4) is a matched asymptotic expansion. The local analysis gives the leading term (3.4) of the inner expansion valid near the saddle point. The outer expansion deals with the diffuse flow in the rest of the domain. The head $\phi(\mathbf{x})$ has, therefor, the form of an inner layer in the direction of the saddle, the x direction in this case.

The head gradient is

$$\nabla\phi \approx -\frac{2C}{\sqrt{\frac{2\pi}{k}}\epsilon} e^{-\frac{k(x-x_s)^2}{2\epsilon^2}} \mathbf{e}_1 \tag{3.5}$$

and the flux is given by

$$\mathbf{j} = -K\nabla\phi \approx K(\mathbf{x}_S)\sqrt{\frac{k}{p}} \frac{2C}{\sqrt{\frac{2\pi}{p}}\epsilon} e^{-\frac{p(y-y_s)^2}{2\epsilon^2}} \mathbf{e}_1 . \tag{3.6}$$

We see from these expressions that when the contrast of $K(\mathbf{x})$ is high (ϵ is small) both the flux and the head gradient are narrow Gaussians centered at $\mathbf{x}_S$, which means that there is strong flow concentration around the saddle point of the conductivity. If there is only one saddle point of $K(\mathbf{x})$ in the domain, the results (3.5) and (3.6) imply that the overall, or effective, conductivity given by (3.1) is (see [11, 5])

$$\overline{K} \approx K(\mathbf{x}_S)\sqrt{\frac{k}{p}}. \tag{3.7}$$

Thus, the flow through the medium can be approximated by the flow through a network consisting of one channel (resistor) with resistance

$$\overline{R} \approx \frac{1}{K(\mathbf{x}_S)}\sqrt{\frac{p}{k}}. \tag{3.8}$$

In more general situations, where there are more saddle points of K in Ω that are oriented in arbitrary directions, the flow still concentrates at the saddles but it follows a more complicated pattern, which is a network of channels (resistors). Locally, around each saddle point of the conductivity, the flow is approximated by the current through a resistor given by (3.8). These resistors are connected in a network that is identified as follows: the nodes of the network are the maxima of $K(\mathbf{x})$ and the branches are paths connecting two adjacent maxima over a saddle point. A detailed analysis is given in [5]. The asymptotic results summarized in this section

were derived for two-dimensional flows. However, the theory can easily be extended to three dimensions (see [11, 5]) so the ideas presented in this paper apply to three-dimensional flow problems as well.

The asymptotic network theory reviewed in this section is only for isotropic media. High contrast anisotropic media, where we may have layers of very different conductivity or fractures, have not been studied, yet.

3.2 The hybrid method

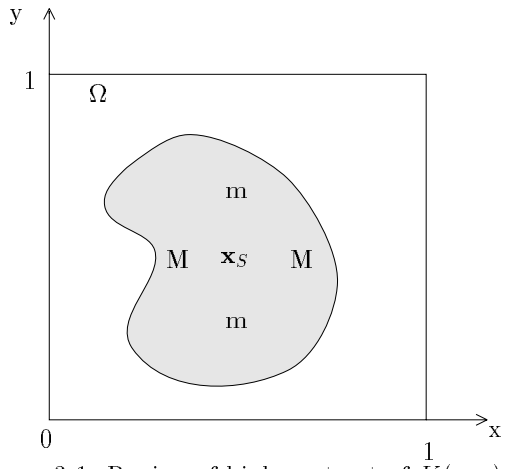

Figure 3.1: Region of high contrast of $K(x, y)$ in Ω

The method we introduce in this section uses the asymptotic result (3.4) in regions of strong flow concentration and matches it with the numerically computed solution elsewhere in the flow regime. The diffuse flow away from the channels can be computed with any standard numerical scheme but for simplicity we choose a second order finite difference method [14]. Thus, we introduce a uniform mesh with spacing $h = 1/N$ and grid points

$$(i, j) \to x_i = (i-1)h, \qquad y_j = (j-1)h, \qquad i, j = 1, \ldots N+1. \tag{3.9}$$

We use the notation

$$\begin{aligned} \phi_{i,j} &= \phi(x_i, y_j), \\ K_{i,j} &= K(x_i, y_j), \\ f_{i,j} &= f(x_i, y_j). \end{aligned} \tag{3.10}$$

and discretize equation (2.1) with a central difference scheme as

$$\begin{aligned} K_{i,j} \frac{(\phi_{i-1,j} + \phi_{i,j-1} - 4\phi_{i,j} + \phi_{i,j+1} + \phi_{i+1,j})}{h^2} \\ + \frac{(K_{i+1,j} - K_{i-1,j})}{2h} \frac{(\phi_{i+1,j} - \phi_{i-1,j})}{2h} + \\ \frac{(K_{i,j+1} - K_{i,j-1})}{2h} \frac{(\phi_{i,j+1} - \phi_{i,j-1})}{2h} = -f_{i,j}. \end{aligned} \tag{3.11}$$

At the boundaries $i = 1$ or $N + 1$ and $j = 1$ or $N + 1$ we have from (2.2)

$$\begin{aligned} \frac{\phi_{2,j} - \phi_{0,j}}{2h} = 0, \qquad \frac{\phi_{N+2,j} - \phi_{N,j}}{2h} = 0, \\ \frac{\phi_{i,2} - \phi_{i,0}}{2h} = 0, \qquad \frac{\phi_{i,N+2} - \phi_{i,N}}{2h} = 0. \end{aligned} \tag{3.12}$$

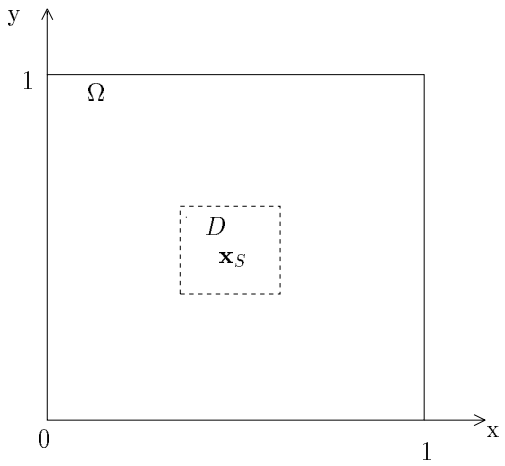

Figure 3.2: Modified numerical domain

We first explain the hybrid method in the simple case shown in fig. 3.1. We assume that the conductivity function has a high contrast region inside Ω (shaded region in fig. 3.1) where $K(x, y)$ has only one saddle point $\mathbf{x}_S$, two minima and two maxima denoted by m and M, respectively. If the contrast in the shaded region is very high, we can assume that $K(\mathbf{x}) = K_0 exp(-\frac{S(\mathbf{x})}{\epsilon^2})$ as explained in the introduction.

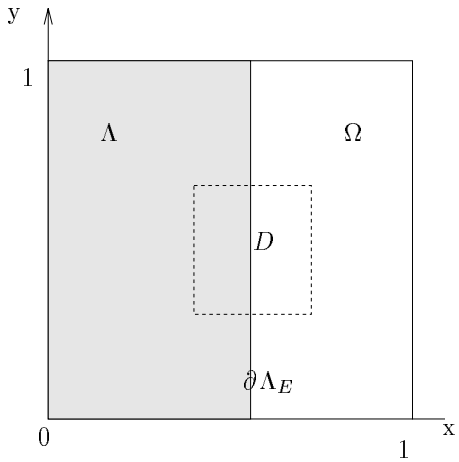

Figure 3.3: The flux in domain D is matched with the flux in $\Omega \setminus D$ across $\partial\Lambda_E$

We define the modified domain $\Omega \setminus D$ as shown in fig. 3.2. Inside the small box D centered at the saddle point, the head $\phi(x, y)$ has the expression (3.4). The constant C quantifies the flux through the saddle point and is treated as an unknown. To compute C beforehand, we would need the effective conductivity for the smooth regions of K, which is clearly unknown, and thus we must compute C numerically. The hybrid method solves (2.1) in $\Omega \setminus D$ with Neumann boundary conditions (2.2) at the outer boundary and Dirichlet boundary conditions (3.4) at the inner boundary. The numerical method used in our computations is the finite difference scheme described at the beginning of this section but clearly, any standard numerical method will do. In order to have an even determined system of equations, an additional equation is needed. This additional equation determines the flux constant C in terms of the nodal values of the head ϕ. We note that if we integrate (2.1) over the shaded region Λ shown in figure 3.3, we obtain

$$-\int_{\Lambda} \nabla \cdot (K\nabla\phi) d\mathbf{x} = -\int_{\partial\Lambda_E} (K\nabla\phi) \cdot \mathbf{e}_1 dy = \int_{\Lambda} f(x, y) d\mathbf{x}, \tag{3.13}$$

which we take as the additional equation needed. The discretization of this equation is done with the trapezoidal rule for integration. We thus obtain a linear system of equations with unknowns $\phi(x_i, y_j)$, $(x_i, y_j) \in \Omega \setminus D$ and the flux C which we solve with a direct solver for banded matrices (see [13]).

3.3 Choosing the size of the inner box

The accuracy of the hybrid method depends on an appropriate choice of the size of the inner box D (see fig. 3.2). Inside the box we assume that the asymptotic approximation (3.4) is accurate. Thus, it is important that D be small enough so that the asymptotic form (3.4) is valid. However, the box cannot be too small because the standard numerical method used in $\Omega \setminus D$ cannot handle well the abrupt change in the head ϕ that occurs in the vicinity of the saddle. Thus, the size of the inner box D must be chosen so as to balance these two conflicting demands.

The asymptotic approximations (3.5) and (3.6) for the head gradient and flux suggest a good guess for the size of D. Both $\nabla\phi$ and $\mathbf{j}$ are Gaussians centered at the saddle point. It is known that at a distance equal to three standard deviations, the Gaussian is basically zero. Since we must match the flux entering D with the one inside, the box should be smaller than this. In fact, numerical experiments show that the appropriate size of the box is close to two standard deviations. Thus, we determine initially the inner box D by

$$\sqrt{\frac{k}{2\epsilon^2}} \mid x - x_s \mid = 2, \qquad \sqrt{\frac{p}{2\epsilon^2}} \mid y - y_s \mid = 2. \tag{3.14}$$

With this choice for D, we compute the flux constant C from equation (3.13). It is important to note that C is obtained by matching the flux across a line that passes through the saddle point (see fig. 3.2). At $x = x_S$, expression (3.4) for the head $\phi(\mathbf{x})$ is very accurate and the computation of C is not affected by a small error in the size of the box. However, the size of the box affects the flux close to the boundaries of D.

We adjust iteratively the size of the inner box from the initial guess (3.14) to a more accurate value by requiring that the flux entering D equals the flux at $x = x_S$ which is known from the previous computation of C. Let us assume that the correct size of the box in the flow direction is

$$\sqrt{\frac{k}{2\epsilon^2}} \mid x - x_s \mid = 2 + \delta, \tag{3.15}$$

where δ is the unknown adjustment parameter. When the inner box size is chosen well, the integrated horizontal flux across the vertical line $x = x_L = x_s - (2+\delta)\sqrt{\frac{2\epsilon^2}{k}}$ satisfies an equation

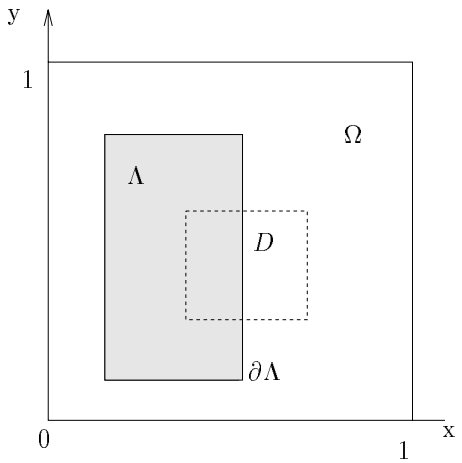

Figure 3.4: Example of an integration domain needed for flux matching in a problem with Dirichlet boundary conditions

similar to (3.13). Thus, we have

$$-\int_{\sqrt{\frac{p}{2\epsilon^2}}|y-y_s|>2} K(x_L,y)\nabla\phi(x_L,y)\cdot\mathbf{e}_1 dy \quad + \quad \int_{\sqrt{\frac{p}{2\epsilon^2}}|y-y_s|\le 2} K(x_L,y)\frac{2C}{\sqrt{\frac{2\pi}{k}}\epsilon}e^{-(2+\delta)^2}dy = \int_0^{x_L}\int_0^1 f(x,y)dxdy, \tag{3.16}$$

where we used the asymptotic result (3.5) for the head gradient and equation (3.15). We now compute δ iteratively by using Newton's method for the nonlinear equation (3.16). The value of the adjustment parameter at iteration $k+1$ is given by

$$\delta^{k+1} = \delta^k + \frac{1}{2(2+\delta^k)}[1 - e^{(2+\delta^k)^2}\frac{\int_0^{x_L}\int_0^1 f(x,y)dxdy + \int_{\sqrt{\frac{p}{2\epsilon^2}}|y-y_s|>2} K(x_L,y)\nabla\phi(x_L,y)\cdot\mathbf{e}_1 dy}{\int_{\sqrt{\frac{p}{2\epsilon^2}}|y-y_s|\le 2} K(x_L,y)\frac{2C}{\sqrt{\frac{2\pi}{k}}\epsilon}dy}]$$

$$\text{where} \quad k = 0,1,2,\ldots \quad \text{and} \quad \delta^0 = 0. \tag{3.17}$$

This Newton iteration converges very fast (two or three steps) because the initial guess (3.14) is very good. Our numerical experiments show that for contrasts of $K(\mathbf{x})$ in the range 10^2 to 10^7, the appropriate size of the box corresponds to (3.14) or $\delta = 0$. Another interesting aspect that comes out of the numerical experiments is that the vertical size of D given by (3.14) is appropriate for all contrasts higher than $O(10^2)$. However, in case an adjustment is needed, one can use a method similar to the above.

3.4 Generalization to arbitrary boundary conditions and multiple channels

In general, when other than Neumann boundary conditions are prescribed along $\partial\Omega$, the computation of the flux constant C in the inner box D cannot be done in a single step (as shown in §3.2). In such situations, C can be obtained iteratively. We can always obtain a good guess

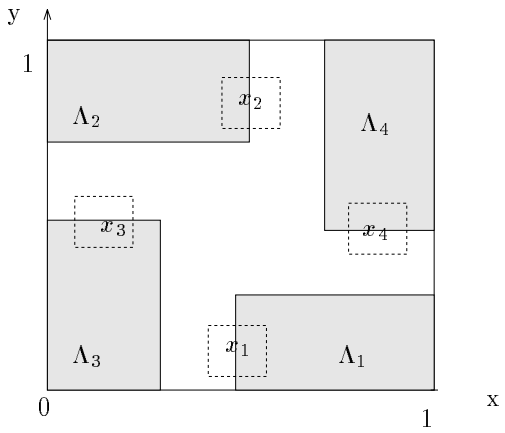

Figure 3.5: Modified Domain (four channels) with regions needed for flux matching

for the initial C by assuming that all the flow passes through the saddle. Then, we improve it iteratively by requiring that the divergence theorem in a domain such as Λ shown in fig. 3.4 be satisfied. Thus, we must have

$$\int_{\Lambda} f(x,y)dxdy = -\int_{\partial\Lambda} K\nabla\phi \cdot \mathbf{n} ds, \tag{3.18}$$

where $\mathbf{n}$ is the outward normal to $\partial\Lambda$. For the portion of $\partial\Lambda$ included in D we use the asymptotic expression (3.5) of the head gradient, and after discretizing (3.18), we obtain a nonlinear equation in C that we solve with Newton's method. Our numerical experiments show very quick convergence (less than five iterations) for contrasts of $K(\mathbf{x})$ that are higher than $O(10^2)$. This is, of course, because we have a good initial guess for the flux constant C.

The hybrid method can be generalized to any number of saddle points and arbitrary orientation of the channels. We illustrate the generalization by considering a conductivity function that has two saddle points $\mathbf{x}_1$ and $\mathbf{x}_2$ in the horizontal direction and two saddle points $\mathbf{x}_3$ and $\mathbf{x}_4$ in the vertical direction. The modified domain used for the numerical computations is shown in figure 3.5 where the shaded regions are the domains of integration for the four additional equations (similar to (3.13)) needed to determine the fluxes through each channel.

4 Performance of the hybrid method

In this section we present results of numerical computations that test the performance of the hybrid method. In our tests we consider media with high contrast hydraulic conductivity that have one or four channels of flow, as described in §3.2. For comparison we also solved the flow problem (2.1)-(2.3) with two additional numerical methods.

One is a standard second order finite difference scheme which uses a uniform discretization of the whole domain Ω. We expect that the performance of this method will be rather poor because the regions of flow channeling need a very fine discretization in order to capture the correct behavior of the solution. Thus, the scheme must use a very fine mesh which leads to an extremely large and ill conditioned matrix that must be inverted. We include in this section the experiments performed with this numerical scheme in order to point out its shortcomings.

The other method used for comparison is PLTMG (see [2]), a carefully designed general purpose solver for elliptic partial differential equations. This is a multigrid solver with a finite

Hybrid M.	Finite Diff.	PLTMG
$h = \frac{1}{32}$	$h = \frac{1}{64}$	$h_{max} = \frac{1}{32}$; $h_{min} = \frac{1}{256}$

Table 4.1: Numerical grids

element discretization based on continuous piecewise linear triangular elements and it provides for adaptive mesh refinement. Even though this solver performs much better than the second order finite difference scheme, we will show that in some cases it does not solve correctly the problem in the high contrast regions of the conductivity. In fact our hybrid solver can be used to estimate the limitations of PLTMG in high contrast situations.

4.1 One region of high contrast

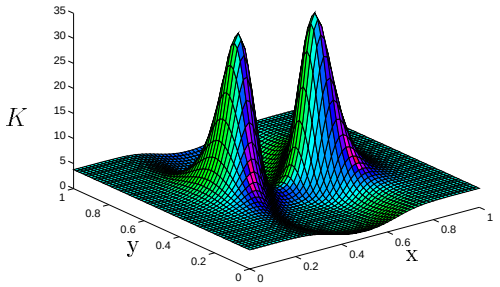

Figure 4.1: Conductivity function

In this section we assume that the conductivity has a single channel (saddle point) of flow concentration (see fig. 4.1). The saddle point is located at $(0.5, 0.5)$ and oriented in the x direction, and the high contrast region of $K(\mathbf{x})$ is embedded in a fairly flat background. We tested the performance of the hybrid method for constant curvatures at the channel ($k = 86.76$, $p = 59.95$), fixed positions of the source (at $(0.2, 0.2)$) and sink (at $(0.8, 0.8)$) and different contrasts ranging from 10^2 to 10^8. The grids used in the computations are described in table 4.1.

The flow computed with the hybrid method for a contrast $\max(K)/\min(K) = 10^4$ is shown in fig. 4.2 and the strong flow concentration in the channel is evident. In order to test our method quantitatively, we looked at the net horizontal and vertical fluxes that can be obtained analytically from (2.1)-(2.3). Thus, we must have

$$\chi(x) = \int_0^1 \mathbf{j} \cdot \mathbf{e}_1 dy - \int_0^1 dy \int_0^x d\xi f(\xi, y) = 0. \tag{4.1}$$

and

$$\Delta(y) = \int_0^1 \mathbf{j} \cdot \mathbf{e}_2 dx - \int_0^1 dx \int_0^y d\eta f(x, \eta) = 0, \tag{4.2}$$

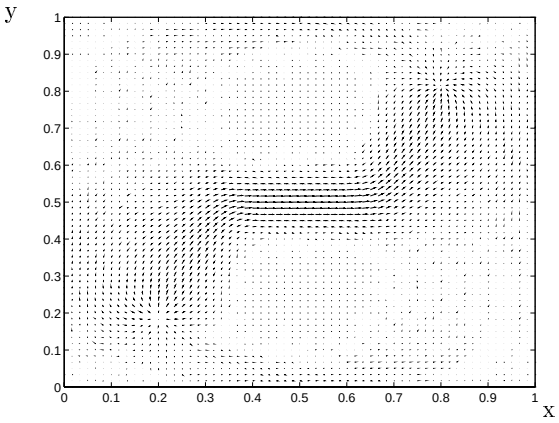

Figure 4.2: Source / sink at $(0.2, 0.2)$ and $(0.8, 0.8)$, Contrast 10^4

where

$$\int_0^1 \mathbf{j} \cdot \mathbf{e}_1 dy = \begin{cases} 0 & if \quad x < 0.2 \quad or \quad x > 0.8 \\ 1 & \text{otherwise} \end{cases} \tag{4.3}$$

and

$$\int_0^1 \mathbf{j} \cdot \mathbf{e}_2 dx = \begin{cases} 0 & if \quad y < 0.2 \quad or \quad y > 0.8 \\ 1 & \text{otherwise.} \end{cases} \tag{4.4}$$

Since in our numerical computations the sources were not delta functions but rather very narrow Gaussians, the net horizontal and vertical fluxes should be smoothed versions of (4.3) and (4.4).

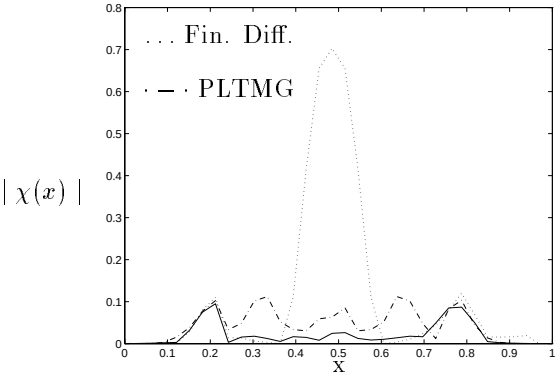

Figure 4.3: Error in the net horizontal flux for contrast 10^4

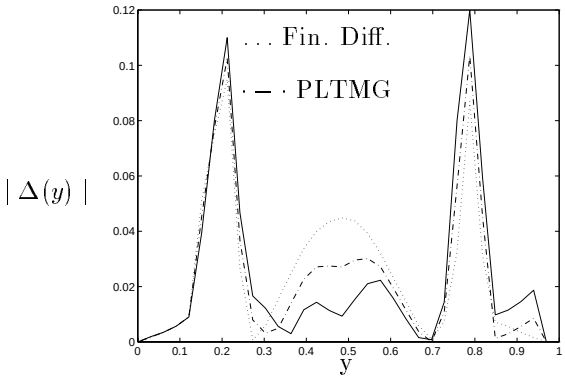

Figure 4.4: Error in the net vertical flux for contrast 10^4

In fig. 4.3 we plot the absolute error in the horizontal flux $|\ \chi(x)\ |$ obtained with the three different numerical methods for a contrast 10^4. The solid line corresponds to the hybrid method, the dotted line to the finite difference method and the dash-dot line to the PLTMG solver. The error given by all three methods is large (absolute error ~ 0.1, relative error $\sim 20\%$) around the "point" source and sink. Slightly away from the sources the hybrid method gives a very good result (the absolute and relative error is less than 0.03), whereas the finite difference method has an error of 70% near the channel. PLTMG gives an error $\chi(x)$ that has an oscillatory behavior in the high contrast region of $K(\mathbf{x})$ (relative error $\sim 13\%$). The solution computed by PLTMG

required an adaptively refined mesh with 5100 vertices. Thus, even though the error given by PLTMG does not seem too bad, the computational cost was much higher than the cost of the hybrid method. Since in our example flow channeling occurs only in the horizontal direction, the net vertical flux computed by all three methods is quite accurate (slightly away from the sources), as can be seen from fig. 4.4.

The performance of the hybrid method remained unchanged for contrasts in the range 10^2 to 10^8 whereas the other two methods performed much better (worse) for contrasts lower (higher) than 10^4. We also tested the hybrid method for different positions of the source and sink and found that its performance is independent of the location of the source and sink provided that they are not in an ϵ neighborhood of the saddle point. In contrast, PLTMG gave quite inaccurate solutions (relative error $\sim 70\%$) when the source or sink were close to the channels and in some situations it failed to converge. Our experiments show that PLTMG gives accurate solutions and uses reasonable meshes for contrasts no higher than $O(10^2)$ provided that the sources are far enough from the channel. The finite difference method requires very fine meshes in order to improve its results ($h \sim 1/200$ for contrast $\sim 10^3$) and is therefore quite inefficient.

We also tested the numerical convergence of the hybrid method for a variety of contrasts in the range 10^2 to 10^8. For example, in an experiment with a contrast of 10^6 and the same curvatures as before, we solved the problem with the hybrid method on two numerical grids. The coarse grid had spacing $h_c = 1/44$ and the fine grid had a double number of grid points (i.e., $h_f = 1/88$). The flux constant C computed on the coarse grid is $C = 0.1093711$ and the fine grid solution is $C = 0.110325$, which corresponds to a relative error of 0.86%. The solution ϕ_f computed on the fine grid is also very close to the coarse grid solution ϕ_c. To be precise, the relative error is $\max_{x \in \Omega} \mid \frac{\phi_c - \phi_f}{\phi_f} \mid = 2.85\%$. Similar results hold for different contrasts of the conductivity $K(\mathbf{x})$.

4.2 Four regions of high contrast

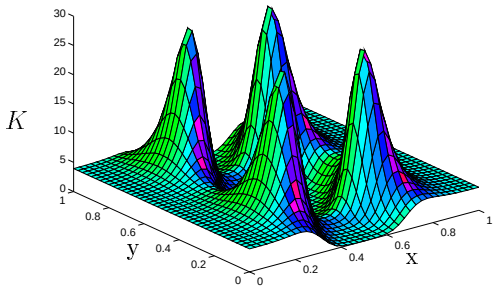

Figure 4.5: The conductivity

In this section we consider media with high contrast hydraulic conductivity that have four channels of flow (saddle points) of $K(\mathbf{x}_S)$. The channels are located at $\mathbf{x}_1 = (0.5, 0.225)$, $\mathbf{x}_2 = (0.5, 0.775)$, $\mathbf{x}_3 = (0.225, 0.5)$ and $\mathbf{x}_4 = (0.775, 0.5)$. Two channels (at $\mathbf{x}_1$, $\mathbf{x}_2$) are horizontal and the other two are vertical. The curvatures of the saddles in the x direction are $k = 99.3$ and $p = 75.4$ and the curvatures of the saddles in the y direction are $k = 11.9$ and $p = 8.12$. The conductivity used in the computations is similar to the one shown in fig. 4.5, but we vary the contrast ($\max(K)/\min(K)$). We tested the performance of the hybrid method for different

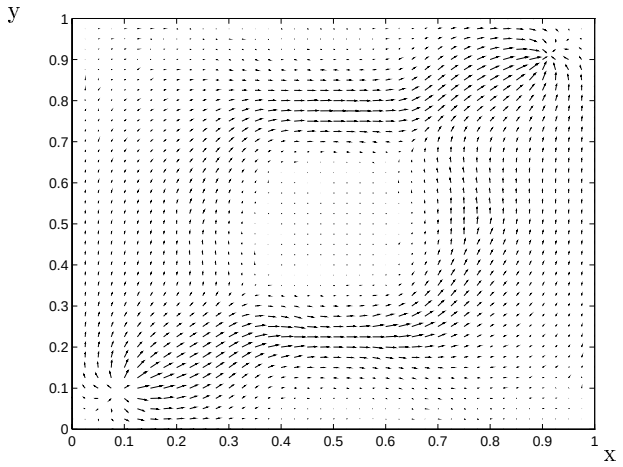

Figure 4.6: Source / sink at $(0.1, 0.1)$ and $(0.9, 0.9)$, Contrast 10^6

contrasts ranging from 10^2 to 10^8 while the position of the source (at $(0.1, 0.1)$) and sink (at $(0.9, 0.9)$) were kept constant. The numerical grids used by the three methods have the same description as before (see table 4.1) and the size of the four inner boxes was chosen according t o (3.14).

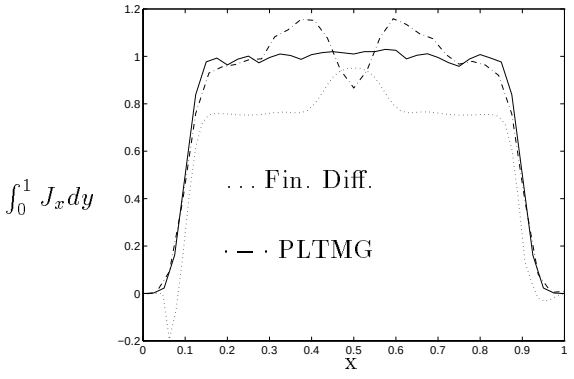

Figure 4.7: Source / sink at $(0.1, 0.1)$ and $(0.9, 0.9)$, Contrast 10^6

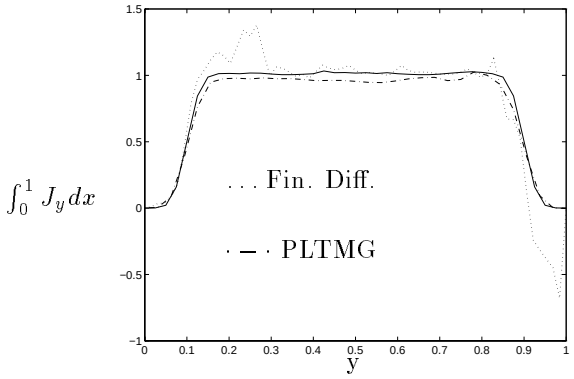

Figure 4.8: Source / sink at $(0.1, 0.1)$ and $(0.9, 0.9)$, Contrast 10^6

The flow computed with the hybrid method for an overall contrast $\max(K)/\min(K) = 10^6$ is shown in fig. 4.6 and it is strongly concentrated in the horizontal channels and only weakly concentrated in the vertical channels that are quite shallow. The error in the vertical and horizontal fluxes given by the hybrid method was as before $\sim 20\%$ around the sources and very small (relative and absolute error ~ 0.03) elsewhere in the domain. In fig. 4.7 and 4.8 we plot the horizontal and vertical fluxes given by all three methods and note that the hybrid method is more accurate than the other two schemes. The horizontal flux computed by the finite difference method is very inaccurate in the high contrast region and PLTMG produces an undesired oscillatory behavior similar to what we showed in §4.1. The net vertical flux computed by all three methods is more accurate because of the weak concentration near the shallow vertical saddles.

We also tested the hybrid method when the source and sink were displaced and the results reconfirmed the conclusions of §4.1 that the performance of the method is independent of the position of the source and sink provided that they are not very near the channels. The other two methods give quite inaccurate solutions when the source or sink are relatively close to any of the channels. For example, an experiment with contrast 10^6, the source located at $(0.4, 0.4)$ and the sink located at $(0.9, 0.9)$, shows that the error in the horizontal flux given by the finite difference method is $\sim 150\%$. The error given by PLTMG is 70%, where an adaptively refined mesh consisting of 6000 vertices was used.

5 Summary and conclusions

We have introduced and tested extensively a hybrid numerical method for solving conductivity problems in a heterogeneous medium with high contrast properties. The method combines analytical results of the asymptotic theory introduced in [11, 5] with the use of a finite difference numerical scheme, but other numerical schemes such as finite elements could also have been used. We carried out extensive numerical tests for different contrasts, different geometries and driving forces and showed that the hybrid method performs much better than standard ones, even the adaptive method of [2] where very fine meshes are used locally. This is not surprising because a general purpose code cannot be expected to do as well as a specially designed method that works for a limited class of problems, like the hybrid method for high contrast media. The use of the hybrid method is restricted to problems with high contrast of the conductivity that arises in a continuum manner, but the ideas presented in this paper can be generalized to any problem where an asymptotically exact solution is known. Our numerical computations show that the performance of the hybrid method is independent of the position of the source or sink in the flow region, except when they are situated very near a saddle point of the conductivity. The other methods have serious difficulties even when the source or sink are not so close to the region of high contrast. The hybrid method performs equally well for contrast of the conductivity ranging from 10^2 to 10^8. The size of the inner box where the asymptotic solution is used is essential for good performance of the hybrid method and the initial choice (3.14) proved to be very good for our computations. The computational cost of the hybrid method is low, hence its efficiency high, because we only discretize the part of the domain where the flow is diffuse and therefore well resolved by standard numerical schemes.

At present, the hybrid method is implemented manually, that is, we must know beforehand the position of the saddle points, their orientation and curvatures which are needed for specifying the saddle boxes.

Acknowledgements

This work was supported by grant AFF49620-94-10436 from AFOSR and by the NSF, DMS 96228554. We wish to thank Peter K. Kitanidis for his interest in our work and many useful comments in the preparation of this paper.

References

[1] Alumbaugh, D. E., *Iterative Electromagnetic Born Inversion Applied to Earth Conductivity Imaging*, PhD Thesis, Engineering - Material Science and Mineral Engineering, UC Berkeley, 1993.

[2] Bank, E. R. *PLTMG: A Software Package for Solving Elliptic Partial Differential Equations*, SIAM, 1990.

[3] Batchelor, G. K., O'Brien, R. W., *Thermal or electrical conduction through a granular material*, Proc. R. Soc. London A, 1977, 355, pp 313-333.

[4] Bensoussan, A., Lions, J. L., Papanicolaou, G. C., *Asymptotic analysis for periodic structures*, North-Holland, Amsterdam, 1978.

[5] Borcea, L., Papanicolaou G. C., *Network approximation for transport properties of high contrast materials*, to appear in SIAM J. Appl. Math.

[6] Borcea, L., Berryman, J. G., Papanicolaou G. C., *High Contrast Impedance Tomography*, Inverse Problems, 12, 1-24, 1996.

[7] Dykaar, B. B., Kitanidis, P. K., *Determination of the Effective Hydraulic Conductivity for Heterogeneous Porous Media Using a Numerical Spectral Approach. 1 Method* and *2. Results*, Water Resources Research, Vol 28, No 4, pp 1155-1166 and 1167-1178, April 1992.

[8] Golden, K. M., Kozlov, S. M., *Critical path analysis of transport in highly disordered random media*, preprint 1995.

[9] Jikov, V. V., Kozlov, S. M., Oleinik, O. A., *Homogenization of Differential Operators and Integral Functional*, Springer-Verlag, Berlin Heilderberg, 1994.

[10] Keller, J. B., *Conductivity of a Medium Containing a Dense Array of Perfectly Conducting Spheres or Cylinders or Nonconducting Cylinders*, J. Appl. Phys., 34 (4), 1963, pp 991-993.

[11] Kozlov, S. M., *Geometric aspects of averaging*, Russian Math. Surveys 44:2, 1989, pp 91-144.

[12] Koplik, J., *Creeping flow in two-dimensional networks*, J. Fluid Mech., 1982, Vol. 119, pp 219-247.

[13] *LAPACK User's Guide,* SIAM, 1992.

[14] Mitchell, A. R., *Computational methods in partial differential equations*, J. Wiley, New York, 1969.